International Journal of Power Electronics and Drive Systems (IJPEDS)
Vol. 14, No. 3, September 2023, pp. 1382~1393
ISSN: 2088-8694, DOI: 10.11591/ijpeds.v14.i3.pp 1382-1393

Fault tolerant control for DFIG wind turbine controlled by ADRC and optimized by genetic algorithm

Ikram Aissaoui[1], Noureddine Elmouhi[1,2], Ahmed Essadki[2], Hind Elaimani[1,2]
[1]Research Center of Engineering and Health Sciences and Technologies (STIS), Ecole Nationale Supérieure d'Arts et Métiers (ENSAM), Mohammed V University, Rabat, Morocco
[2]Laboratory of Innovation in Management and Engineering for Enterprise (LIMIE), Institut Supérieur d'Ingénierie et des Affaires (ISGA Rabat), Rabat, Morocco

Article Info

Article history:

Received Apr 19, 2022
Revised May 1, 2023
Accepted May 12, 2023

Keywords:

ADRC
DFIG
Fault tolerant control
Genetic algorithm
Wind turbine

ABSTRACT

This research work deals with the modelling, control and simulation of a wind turbine based on the doubly fed induction generator (DFIG) in the current sensor's failure event. We present in the first time the model of the wind energy conversion system based on the DFIG and the control by active disturbances rejection control (ADRC) optimized by genetic algorithm. Particular focus is directed towards on a technique for detection, identification, isolation and reconfiguration of current sensor signals after failure. The combination of the two preceding techniques makes it possible to have a fault tolerant control to sensor faults which ensures continuity of service in all circumstances. The robustness of the proposed technique is tested under the MATLAB/Simulink environment.

Corresponding Author:

Noureddine Elmouhi
Research Center of Engineering and Health Sciences and Technologies (STIS)
Ecole Nationale Supérieure d'Arts et Métiers (ENSAM), Mohammed V University
Rabat, Morocco
Email: n.elmouhi@gmail.com

NOMENCLATURE

Φrdq	: Rotor fluxes
Vsdq	: Stator voltages dq axis
Vrdq	: Rotor voltages dq axis
isdq	: Stator currents dq axis
irdq	: Rotor currents dq axis
ωs	: Rotor angular frequency
ωr	: Stator angular frequency
Φrdq	: Rotor fluxes

1. INTRODUCTION

A real system during its operation can be impacted by faults, which generates a deviation from its normal operation and can cause its instability depending on the fault severity [1]. The variable speed electric drives that exist in wind power generation systems are equipped with sensors either for their protection or for their control [1]. In doubly fed induction generator (DFIG) based wind energy conversion systems, we often find current sensors for the stator and rotor currents, a voltage sensor for measuring the DC link voltage and optionally a speed or position sensor depending on the performance level required by the control method used [1], [2].

The performance level of the DFIG control relies particularly on the quality and accuracy of the feedback signal from the sensors. However, sensors can be weak links in the control loop [3]. The sensor fault would cause a malfunction of the control and lead in most cases to the system shutdown and the wind turbine disconnection.

Nevertheless, a shutdown results in a shutdown of the production system and therefore in a loss of an electrical energy quantity. This is more impacting as the requirements of electric grid managers are greater [4]. So, the development of a fault tolerant control therefore becomes more and more necessary and inevitable.

The DFIG control based on the active disturbances rejection control (ADRC), unlike other control techniques, makes it possible to compensate, in real time, internal and external disturbances, in particular those linked to the controller's sensitivity to parameters' variations of the generator [5]. This control technique has proven its effectiveness and robustness in several works but it requires reliable and precise measurement of rotor and stator currents to guarantee the wind system stability and precision. However, it does not take into account the sensors' faults which must be treated separately [1], [2].

Several works have dealt with the detection and isolation of sensor faults to improve the DFIG control robustness to the current sensors failure as well as increasing the quality of the electrical energy produced. The proposed method by Rothenhagen and Fuchsin [6] is based on an bilinear observer current to generate necessary residuals for the detection and reconfiguration of the current signals after one of the current sensors' failure. The disadvantage of this method is that the observer synthesis is based on the output currents of the same faulty sensor, which can make the values generated by the observer also erroneous and sensitive to the faulty sensor.

Gálvez-Carrillo and M. Kinnaert [7] have dealt with fault detection and isolation in current and voltage sensors of doubly-fed induction generators. The presented approach in this work for the fault's detection requires more time and entails many difficulties to have a fault tolerant control practically. The studies deal only with the case of a serious fault for the sensors in the DFIG. The work presented in [8] deals with fault-tolerant control of sensors using a Luenberger observer for the current's estimation. The control assumes a fixed wind speed.

In this work, we propose an active control based on ADRC optimized by genetic algorithm to control the active and reactive powers of DFIG, combined with a fault tolerant control which allows to compensate different types of current sensor faults, including gain, offset and open circuit faults for a variable wind speed. It is based on a current's estimator using a nonlinear model representation of the DFIG, by using only voltage signals as inputs. The estimated currents will be compared to the currents measured by the sensors and then fed into an algorithm for fault isolation and signal reconfiguration. We also interested in the robustness test of the proposed control, integrating the block of the rotor current sensor fault diagnostic under a variable wind profile, in the case of a fault impacting the gain, the offset and of the open circuit type.

2. RESEARCH METHOD

2.1. DFIG modeling

The DFIG model is obtained from the dynamic equations of stator and rotor fluxes (1) and voltages (2) in the dq reference [9], [10]:

$$\begin{cases} \Phi_{sd} = L_s i_{sd} + L_m i_{rd} \\ \Phi_{sq} = L_s i_{sq} + L_m i_{rq} \\ \Phi_{rd} = L_r i_{rd} + L_m i_{sd} \\ \Phi_{rq} = L_r i_{rq} + L_m i_{sq} \end{cases} \tag{1}$$

$$\begin{cases} V_{sd} = R_s i_{sd} + \frac{d\Phi_{sd}}{dt} - \omega_s \Phi_{sq} \\ V_{sq} = R_s i_{sq} + \frac{d\Phi_{sq}}{dt} + \omega_s \Phi_{sd} \\ V_{rd} = R_r i_{rd} + \frac{d\Phi_{rd}}{dt} - \omega_r \Phi_{rq} \\ V_{rq} = R_r i_{rq} + \frac{d\Phi_{rq}}{dt} + \omega_r \Phi_{rd} \end{cases} \tag{2}$$

The structure of wind power system based on DFIG is presented in Figure 1. In this block diagram, the DFIG stator is directly connected to the grid and the rotor is connected to the grid through two converters, rotor side converter (RSC) and grid side converter (GSC), and a DC link. Usually, the RSC controls the produced powers, and the GSC controls the DC link voltage [9], [11], [12].

2.2. Active disturbances rejection control

Active disturbances rejection control is a robust control that improves system performances in the presence of disturbances. It is based on the extension of the model system by the use of an extended state observer (ESO) to estimate and cancel, in real time, internal and external disturbances. Figure 2 show the basic structure of ADRC controller [5], [13], [14].

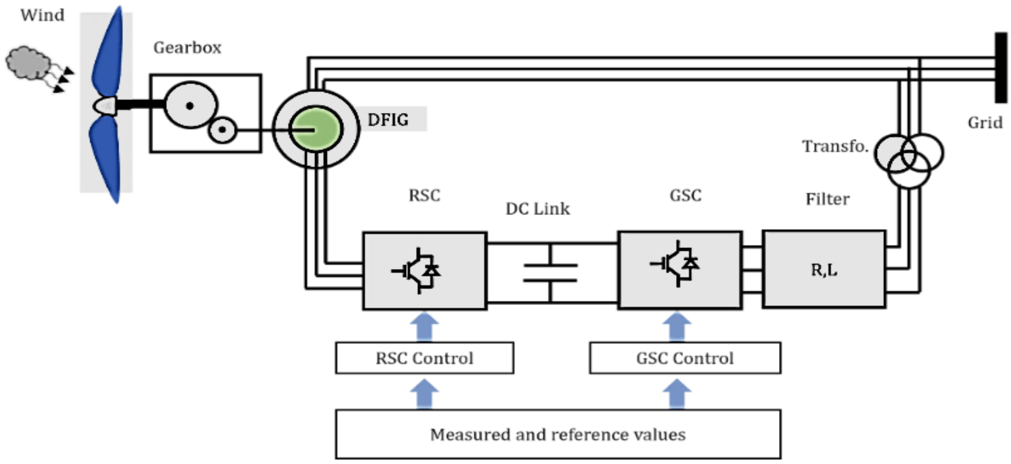

Figure 1. Structure of wind power system based on DFIG

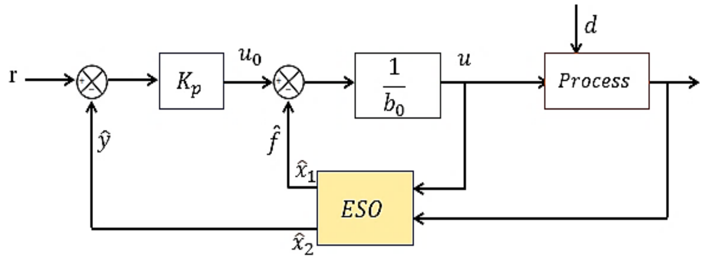

Figure 2. Structure of the ADRC controller

The f represents the total disturbances affecting the controlled quantities on the d and q axes, u is the control input of the loops [13]. $b0$ is the known part of the generator parameters and Kp represent the ADRC controller gain [13].

2.2.1. Rotor side converter control

The form of the dynamic equations of stator and rotor currents and voltages, rotor currents expressions can be expressed to be (3) and (4) [13], [15]:

$$\frac{di_{rd}}{dt} = -\frac{R_r}{\sigma L_r} i_{rd} + \omega_r . i_{rq} + \frac{1}{\sigma L_r} V_{rd} \tag{3}$$

$$\frac{di_{rq}}{dt} = -\frac{R_r}{\sigma L_r} i_{rq} - \omega_r . i_{rd} - \omega_r \frac{L_m}{\sigma L_r L_s} \Phi_s + \frac{1}{\sigma L_r} V_{rq} \tag{4}$$

$\sigma = 1 - \frac{L_m^2}{L_s L_r}$ represent the dispersion coefficient. We can also put these equations as follows:

$$\frac{di_{rd}}{dt} = f_d(i_{rd}, d, t) + b_0 u(t) \tag{5}$$

$$\frac{di_{rq}}{dt} = f_q\left(i_{rq}, d, t\right) + b_0 u(t) \tag{6}$$

where:

$$\begin{cases} f_d = -\frac{R_r}{\sigma L_r} i_{rd} + \omega_r . i_{rq} + (\frac{1}{\sigma L_r} - b_0) V_{rd} \\ \quad u = V_{rd} \;\;,\;\; b_0 = \frac{1}{\sigma L_r} \end{cases} \tag{7}$$

$$\begin{cases} f_q = -\frac{R_r}{\sigma L_r} i_{rq} - \omega_r . i_{rd} - \omega_r \frac{L_m}{\sigma L_r L_s} \Phi_s + (\frac{1}{\sigma L_r} - b_0) V_{rq} \\ \quad u = V_{rq} \;\;,\;\; b_0 = \frac{1}{\sigma L_r} \end{cases} \tag{8}$$

2.2.2. Grid side converter control

The grid filter currents i_{fd} and i_{fq} are given by the following expressions [13], [16], [17]:

$$\frac{di_{fd}}{dt} = \frac{1}{L_f}V_{sd} - \frac{R_f}{L_f}i_{fd} - w_s i_{fq} - \frac{1}{L_f}V_{fd} \tag{9}$$

$$\frac{di_{fq}}{dt} = \frac{1}{L_f}V_{sq} - \frac{R_f}{L_f}i_{fq} - w_s i_{fd} - \frac{1}{L_f}V_{fq} \tag{10}$$

According to the ADRC structure, these expressions can be rearranged to be in the (11) and (12):

$$\frac{di_{fd}}{dt} = f_{fd}\left(i_{fd}, d, t\right) + b_0 u(t) \tag{11}$$

$$\frac{di_{fq}}{dt} = f_{fq}\left(i_{fq}, d, t\right) + b_0 u(t) \tag{12}$$

where:

$$\begin{cases} f_{fd} = \frac{1}{L_f}V_{sd} - \frac{R_f}{L_f}i_{fd} - w_s i_{fq} + (\frac{1}{L_f} - b_0)V_{fd} \\ \qquad u = V_{fd} \ , \quad b_0 = -\frac{1}{L_f} \end{cases} \tag{13}$$

$$\begin{cases} f_{qf} = \frac{1}{L_f}V_{sq} - \frac{R_f}{L_f}i_{qf} - w_s i_{df} + (\frac{1}{L_f} - b_0)V_{qf} \\ \qquad u = V_{qf} \ , \quad b_0 = -\frac{1}{L_f} \end{cases} \tag{14}$$

The i_{fq} and i_{fd} currents are controlled to have a unity power coefficient. The block diagram of the RSC and GSC control is given in Figure 3.

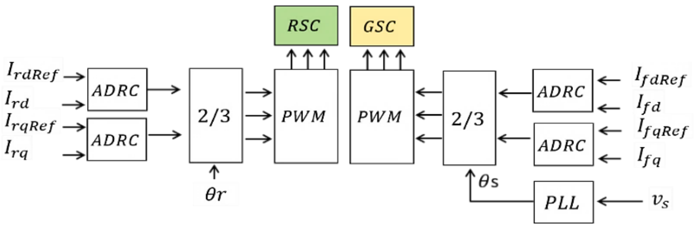

Figure 3. Block diagram of the RSC and GSC control

2.3. Fault tolerant control

For ADRC-based DFIG control, it is often necessary to measure the stator current and rotor current and voltage. So, for current measurement, we can use either three sensors, one for each phase, or only two sensors and calculate the third of the two acquired signals, since the sum of the three currents is zero for a balanced three-phase system [18]–[20].

The Figure 4 shows the synoptic diagram of the rotor side converter control using ADRC integrating the detecting and reconfiguration block for sensor's signals in the faults event. We will detail in the following section the usefulness and operation of each block of the preceding synoptic diagram for currents estimation, detection, isolation and reconfiguration of the signals at the appearance of rotor current faults.

2.3.1. Fault detection

This operation makes it possible to decide whether the system is or is not in a normal operating state. For this, a logic operation is performed, the response of this bloc must be binary (0 if there is no fault and 1 if the system is faulty). The technique is based on the fact that the phases sum of the balanced three-phase system is close to zero [18], [21]. The system is therefore faulty if this sum is greater than a threshold, which will be fixed during simulation, (output at 1) and in normal operation in the other case (output at 0). In Figure 5 we present the fault detection diagram.

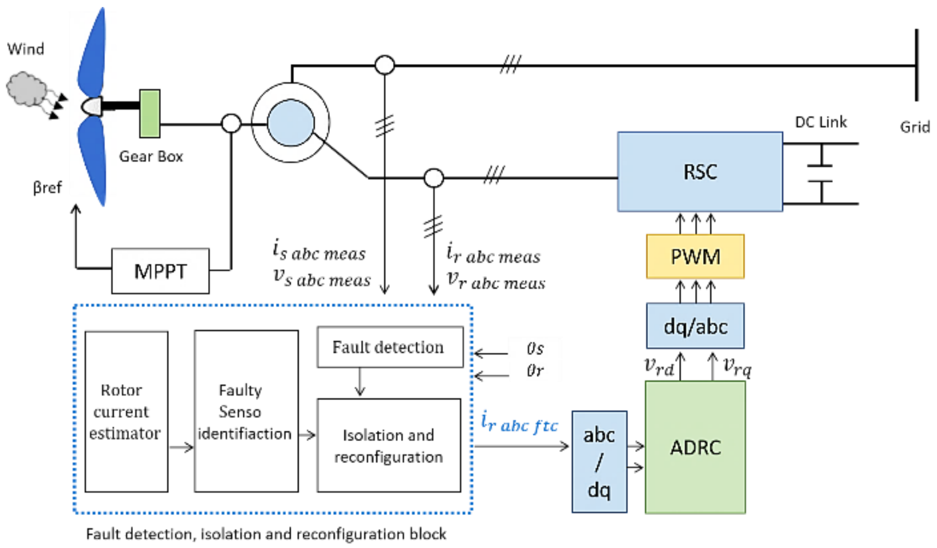

Figure 4. Synoptic scheme of detection, identification, and reconfiguration block

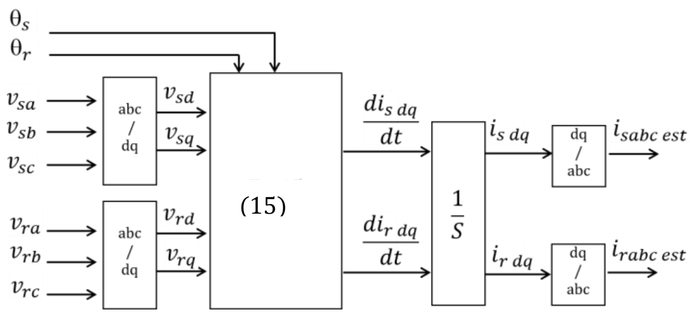

Figure 5. Rotor and stator currents estimation block

2.3.2. Current estimation

The estimation of the stator and rotor currents is based on the measurement of the generator voltages. According to the mathematical equations of the DFIG modelling (voltage and flux), we can write the simplified equations of the DFIG dynamics in the following form (15) [21]–[24]:

$$\begin{cases} \dot{x}_1 = \frac{R_s}{\sigma L_s}x_1 + \left(\omega_s + \frac{L_m^2\omega}{\sigma L_s L_r}\right)x_2 + \frac{R_r L_m}{\sigma L_s L_r}x_3 + \frac{L_m\omega}{\sigma L_s}x_4 + \frac{1}{\sigma L_s}u_1 - \frac{L_m}{\sigma L_s L_r}u_3 \\ \dot{x}_2 = -\left(\omega_s + \frac{L_m^2\omega}{\sigma L_s L_r}\right)x_1 - \frac{R_s}{\sigma L_s}x_2 - \frac{L_m\omega}{\sigma L_s}x_3 + \frac{R_r L_m}{\sigma L_s L_r}x_4 + \frac{1}{\sigma L_s}u_2 - \frac{L_m}{\sigma L_s L_r}u_4 \\ \dot{x}_3 = -\frac{R_s L_m}{\sigma L_s L_r}x_1 - \frac{L_m\omega}{\sigma L_r}x_2 + \frac{R_r}{\sigma L_r}x_3 + \left(\omega_s - \frac{\omega}{\sigma}\right)x_4 - \frac{L_m}{\sigma L_s L_r}u_1 - \frac{1}{\sigma L_r}u_3 \\ \dot{x}_4 = \frac{L_m\omega}{\sigma L_r}x_1 + \frac{R_s L_m}{\sigma L_s L_r}x_2 - \left(\omega_s - \frac{\omega}{\sigma}\right)x_3 - \frac{R_r}{\sigma L_r}x_4 + \frac{L_m}{\sigma L_s L_r}u_2 + \frac{1}{\sigma L_r}u_4 \end{cases} \quad (15)$$

where:

$$x^T = (x_1 x_2 x_3 x_4)^T = \left(i_{sd} i_{sq} i_{rd} i_{rq}\right)^T$$

$$u^T = (u_1 u_2 u_3 u_4)^T = \left(v_{sd} v_{sq} v_{rd} v_{rq}\right)^T$$

The stator voltages are measured by a voltage sensor, and the rotor voltages are obtained directly from the ADRC control blocks presented in the previous section. The Figure 5 summarizes the method used to estimate the stator and rotor currents.

2.3.3. Identification of defective sensors

The identification of the defective sensor is done in two steps: i) Calculation of the difference between the estimated values $i_{rabc\ est}$ and the measured ones $i_{rabc\ meas}$ by the current sensors; and ii) Comparison of this deviation with a threshold to be set during the simulation.

The faulty sensor is identified as follows: If the value of the difference between the estimated value and the measured one is greater than the threshold, the sensor is considered defective and the output variable of the identification block is at logic state 1, otherwise it is at 0. The Figure 6 summarizes the method used to detect the sensor current fault and the fault identification diagram. The threshold must be greater than the maximum difference between the estimated value of the current and the measured one in the normal case without fault. This threshold depends on the precision of the current's estimation method.

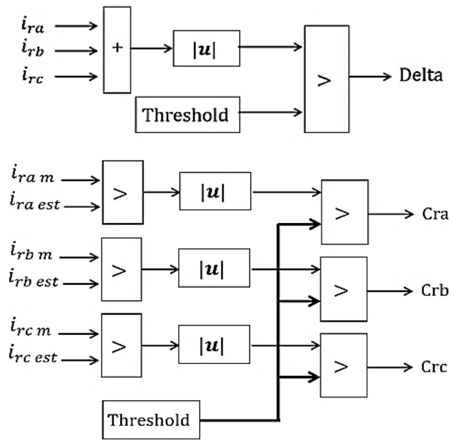

Figure 6. Faulty sensor detection block

2.3.4. Isolation and reconfiguration algorithm

In this part we are interested in the algorithm used for the generation of the currents to be transmitted to the ADRC controllers. For this, we have three cases to tread:

- If all the logic outputs of the detection block are at zero (no fault), the measured values of the currents $i_{rabc\ meas}$ are transmitted directly to the ADRC controllers.
- If only one sensor is faulty, its signal is isolated and reconfigured from the other two sensors (for example $i_{ra\_rec} = -i_{rb\_m} - i_{rc\_m}$ if sensor a is faulty).
- If two or three sensors are defective, the ADRC controllers will receive the generated currents by the estimation block in Figure 5.

Figure 7 summarize the isolation and reconfiguration algorithm presented previously.

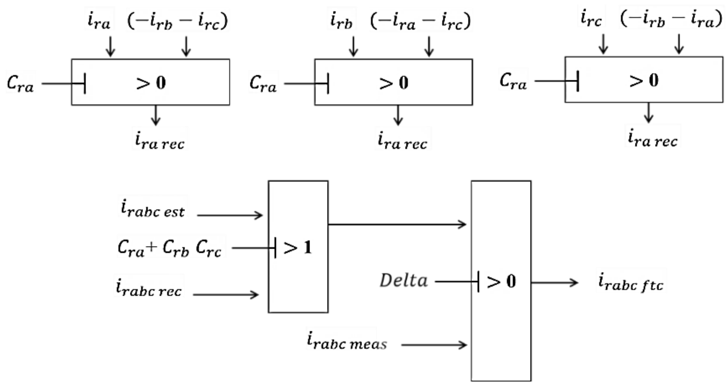

Figure 7. Isolation and reconfiguration diagram

2.4. Optimization by genetic algorithm

The genetic algorithm is an optimization method based on theories of natural selection [25]. This technique is recognized to be very effective and efficient in finding optimal solutions to optimization problems.

It makes it possible to avoid local minima constituting a major problem in the case of nonlinear systems [25]–[27]. In this technique, the solutions to an optimization problem are represented as chromosomes from an initial population to evolve to an optimal solution [26]. This algorithm is based on three stages: selection, crossing and mutation. These three steps are used to have new individuals and subsequently assess their performance against the previous ones using a fitness function [26]. The optimal solution is represented the best individuals, this algorithm must be realized for many generations and finally stops when it reaches these chromosomes [25], [27].

In this research paper, genetic algorithm is used to optimize the DFIG control in the current sensor fault event. It is used to adjust the parameters K_p, β_1 and β_2 for extended state observer so as to obtain the optimal performance in terms of dynamics, robustness and disturbance rejection. The objective function is chosen so that the difference between the reference of active and reactive power and the measured one is as small as possible. The electromagnetic torque produced by DFIG and active stator power are proportional to the rotor current of q-axis. The reactive power is related to current rotor d-axis by a constant imposed by the grid. The (16) and (17) give the expressions of these reference currents:

$$i_{rdref} = \frac{\Phi_s}{L_m} - \frac{L_s}{v_{sq} L_m} Q_{sref} \tag{16}$$

$$i_{rqref} = \frac{2}{3} \frac{L_s}{p L_m \Phi_s} T_{emref} \tag{17}$$

A GA based ADRC optimization block for rotor current's control can be represented in Figure 8. The types of the GA operations used are presented in Table 1. The genetic algorithm parameters used in this work are presented in Table 2. In Figure 9, we present the ADRC parameters' evolution through the generation. From Figure 9, we can deduce the ARDC controller parameters Kp, β1 and β2 which are given in the Table 3.

Table 1. Types of the GA operations used

Property	Type
Selection	GA default selection function
Mutation	Uniformed
Crossover	Arithmetic

Table 2. Genetic algorithm parameters

Property	Value	Property	Value
Variables to optimize	3	Mutation fraction	0.01
Population size	50	Crossover fraction	0.08
Maximum size of generations	500	Tolerance	5.10^2

Table 3. ADRC Controller Parameters

Parameter	Symbol	Value obtained by GA	Lower range	Upper range
Currents controller gain (ADRC)	K_p	18680	1.0	20000
Extended state observer gains	β_1	4524.2	1.0	5000
	β_2	480900	1.0	500000

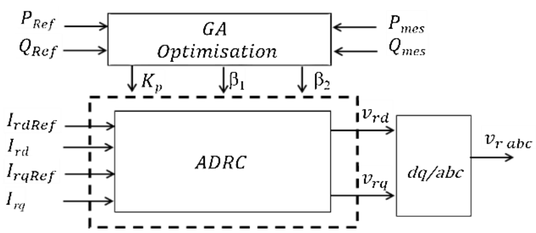

Figure 8. GA based ADRC optimization block

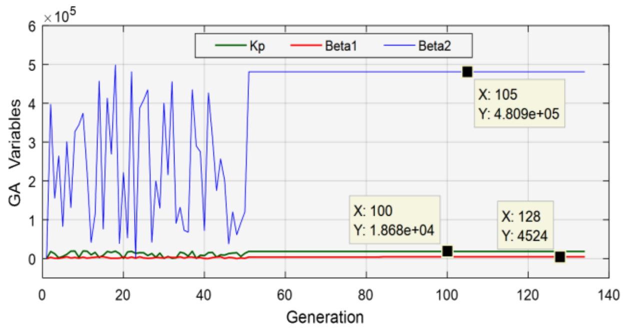

Figure 9. GA parameters' evolution

3. RESULTS AND DISCUSSION

The parameters of a 1.5 MW DFIG, RL filter and the DC link parameters used in the simulation are presented in Tables 4 and 5. Simulation results are divided in two parts, first one tracking and control test, second one verifies fault tolerant control performance. In this research paper, the wind speed profile used is modelled by a sum of several harmonics, around an average speed of 8 m/s. We present in Figure 10 the used wind profile.

Table 4. DFIG parameters

Parameter	Symbol	Value	Parameter	Symbol	Value
Rated power	P_s	1.5 M	Mutual cyclic inductance	L_m	13.5 mH
Stator resistance	Rs	8.9 mΩ	Number of pole pairs	p	2
Rotor resistance	R_r	13.7 mΩ	Optimal tip speed ratio	λopt	8.1
Stator inductance	L_s	13.7 mH	Maximal power coefficient	Cpmax	0.48
Rotor inductance	L_r	13.67 mH			

Table 5. Parameters of the RL Filter and the DC Link

Parameter	Symbol	Value
Filter resistance	R_f	0.25 Ω
Filter inductance	L_f	0.005 H
DC link Capacitor	C	0.0044 F
DC link voltage	U_{dc}	1200 V

3.1. Tracking and control test

As results of tracking and control test Figure 10 shows the simulation result for the active and reactive powers P and Q and the rotor current i_{rabc} of the DFIG, controlled by ADRC without rotor current sensor faults. The reference reactive power is initially chosen equal to 0 VAR to guarantee a unity power factor at the point of connection to the grid.

From Figure 10, the active and reactive powers controlled by ADRC and optimized by genetic algorithm, follow perfectly their references, and the rotor current frequency follow the wind profile considered for this simulation according to the DFIG rotation speed which further demonstrates the effectiveness of the ADRC command used.

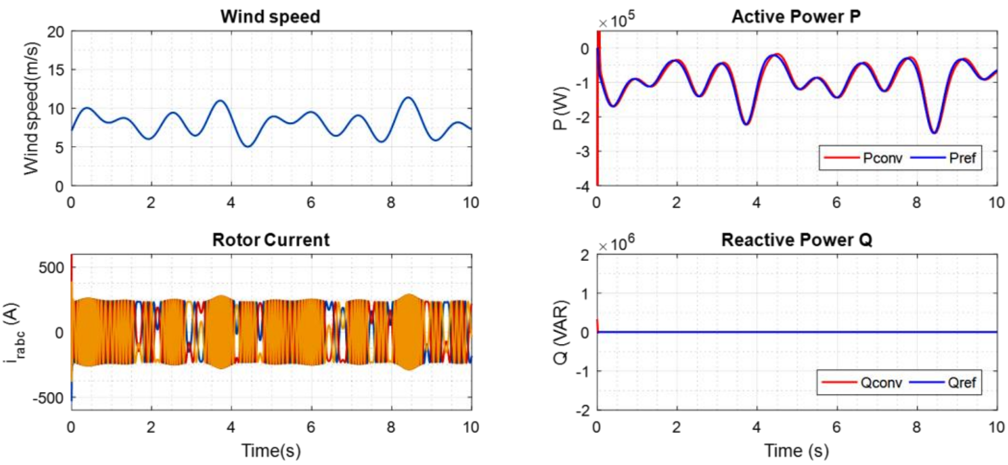

Figure 10. Active and reactive power

3.2. Simulation of fault tolerant control performance

In this section, the performance of the DFIG control by ADRC will be tested with the rotor current estimator in the presence of current sensor faults. The objective is to validate the fault-tolerant control method. For this, we consider two scenarios which will be studied: i) An open circuit fault affecting only phase a between 4s and 6s; and ii) A gain fault of 0.5s applied to phase c between 2.5s and 4.5s, simultaneously with an offset fault affecting phase b between 5.5s and 7s.

According to the reference tracking test validated in the previous part, the system response always passes through a transient state before the steady state is established. This transient state (about 500 ms) causes also a transient state in the currents generated by the rotor current estimator, which is based on the rotor voltages generated by the ADRC controllers. Therefore, the proposed command remains always valid for faults appearing after starting the generator.

In Figure 11, we show the outputs of the residual's calculation block between the measured currents and the estimated currents, and the indicators of the sensor's current faults, obtained during the simulation under the wind speed variations. From this figure, the residual for the current i_{ra} (left figure) is different to zero due to the presence of the open circuit fault on the sensor a. the fault indicator also changes to 1. In the figure on the right, the presence of gain and offset faults generates non-zero values in the residuals Rrb and Rrc and the indicators Crb and Crc changes to 1.

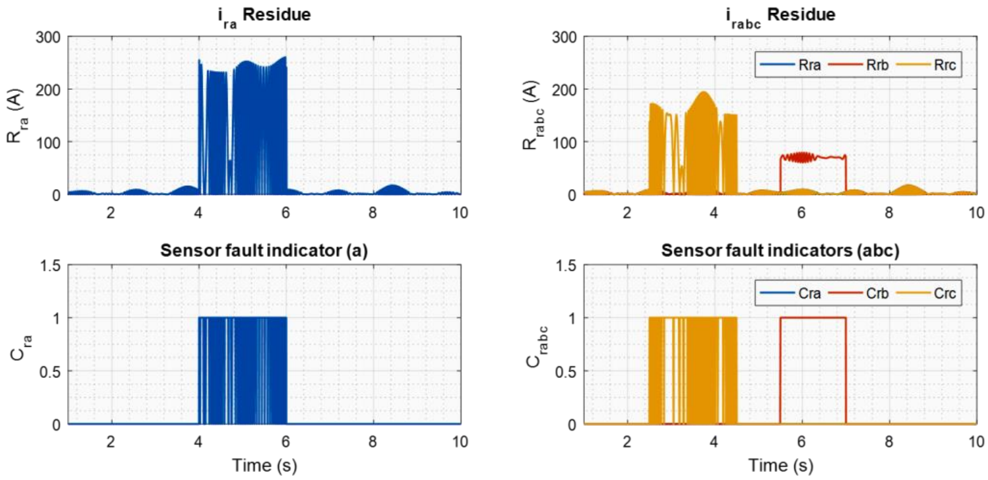

Figure 11. Residuals of rotor current

When all the sensors are in normal operation (indicated by a low state on the Delta outputs of the detection block), the FTC command returns the measured currents to the ADRC controllers. When a fault appears, the identification and reconfiguration block is used to generate the current $i_{r\,abc\,ftc}$. This current is equal either to the reconfigured current if the fault affects a single sensor or estimated one if several sensors are affected. During the start-up regime of the DFIG, the ADRC control block receives the measured current by the sensors.

Figure 12 shows the simulation results obtained for the rotor current in the case of the two scenarios taken as an example. It can be noted, according to this figure, that the first fault (OC open circuit) is applied only to phase a at 4s (i_{ra}). The current detection, estimation and reconfiguration block reacts instantly to isolate the fault and generate the rotor currents. It can be seen from these results that these generated currents are perfectly sinusoidal and conform to the magnitudes without defects (measured current i_{rabc} without fault). We note the same remark for the case of gain and offset fault applied simultaneously at 2.5s and 5.5s.

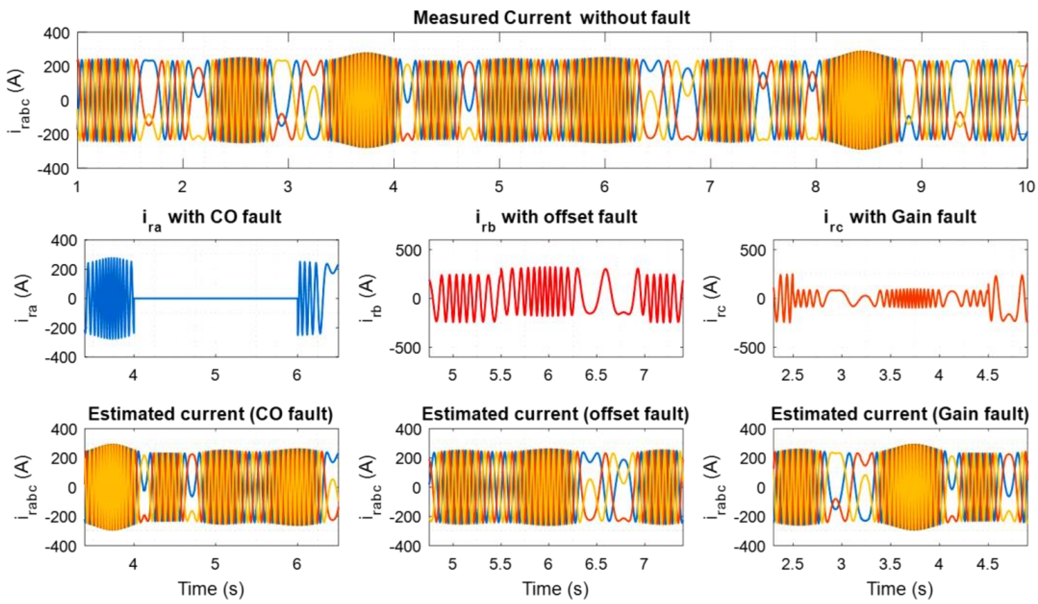

Figure 12. Rotors current with OC fault, offset fault and gain fault

For the active and reactive power P and Q, we can note, according to Figure 13, a strong divergence of these powers with more oscillations in the case of the sensor defect appearance with the conventional method, which does not integrate the reconfiguration technique (Pconv and Qconv). However, the control of these powers by ADRC strategy, integrating the detection and reconfiguration technique of the current sensors signals, Pftc and Qftc, presents better performances in terms of robustness, speed and monitoring of the reference values Pref and Qref. This is valid for the three default scenarios considered.

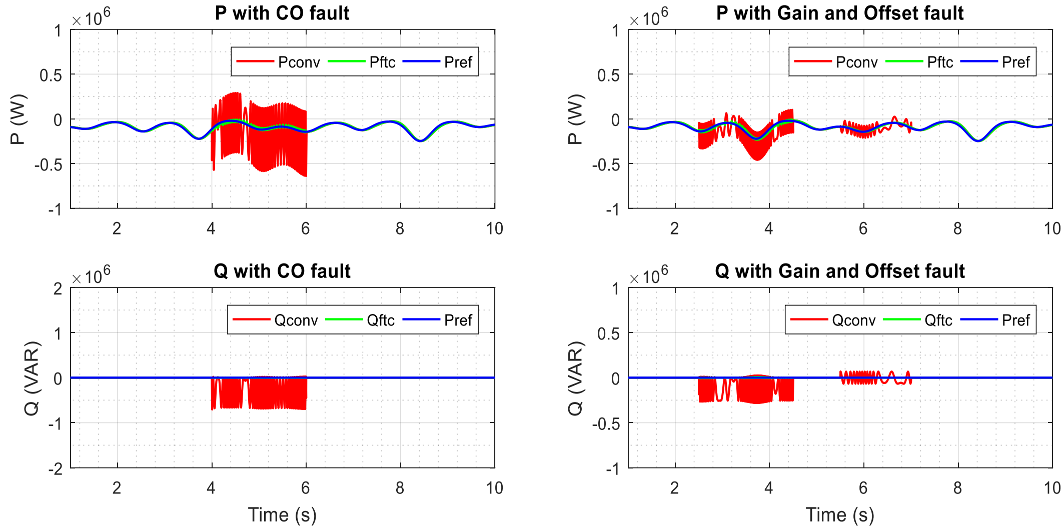

Figure 13. Active and reactive power for OC, offset and gain fault

4. CONCLUSION

This article has dealt with the fault-tolerant control of DFIG current sensors, based on the ADRC technique optimized by genetic algorithm. This method consists of detecting and identifying faults in current sensors, estimating currents and reconfiguring sensor signals. In this work, we considered three types of faults: open circuit fault, offset and gain faults affecting the rotor current sensors. The simulation results obtained showed that the conventional control without a detection faults and signals reconfiguration strategy does not allow the wind energy conversion system, based on DFIG, to ensure the continuity of service in the event of current sensor failure. However, the proposed control makes it possible to detect the faults, identify the faulty current sensor, generate the estimated currents based only on the DFIG voltages and then isolate and reconfigure the signals for the erroneous sensors. The use of the genetic algorithm allowed us to have an optimal solution for the parameters' values of the ADRC controllers. As perspectives, this work can be further improved by considering a robust adaptive observer, based on the genetic algorithm, for rotor and stator currents estimation instead of the state estimator.

REFERENCES

[1] M. Abdellatif, "Continuity of electrical drive's service drives for an induction machine supplied by the stator and the rotor in the presence of sensor faults (in french : Continuité de service des entraînements électriques pour une machine à induction alimentée par le s," Toulouse university, France, 2010.

[2] I. Idrissi, "Contribution to the diagnosis of variable-speed wind turbine faults using a double-fed asynchronous machine," Sidi Mohammed Ben abdellah University, 2019.

[3] A. Al-Ajmi, Y. Wang, and S. Djurović, "Wind turbine generator controller signals supervised machine learning for shaft misalignment fault detection: A doubly fed induction generator practical case study," *Energies*, vol. 14, no. 6, 2021, doi: 10.3390/en14061601.

[4] N. Elmouhi, A. Essadki, H. Elaimani, and R. Chakib, "Participation of a DFIG based wind energy conversion system in frequency control," *2020 5th International Conference on Renewable Energies for Developing Countries, REDEC 2020*, vol. 5, pp. 5–10, 2020, doi: 10.1109/REDEC49234.2020.9163879.

[5] H. Laghridat, A. Essadki, and T. Nasser, "Comparative Analysis between PI and Linear-ADRC Control of a Grid Connected Variable Speed Wind Energy Conversion System Based on a Squirrel Cage Induction Generator," *Mathematical Problems in Engineering*, vol. 2019, 2019, doi: 10.1155/2019/8527183.

[6] K. Rothenhagen and F. W. Fuchs, "Current sensor fault detection, isolation, and reconfiguration for doubly fed induction generators," 2009. doi: 10.1109/TIE.2009.2017562.

[7] M. Gálvez-Carrillo and M. Kinnaert, "Fault detection and isolation in current and voltage sensors of doubly-fed induction generators," 2009. doi: 10.3182/20090630-4-es-2003.00221.

[8] K. Rothenhagen and F. W. Fuchs, "Doubly fed induction generator model-based sensor fault detection and control loop reconfiguration," 2009. doi: 10.1109/TIE.2009.2013683.

[9] N. Elmouhi, A. Essadki, H. Elaimani, and R. Chakib, "Evaluation of the inertial response of variable speed wind turbines based on DFIG using backstepping for a frequency control," 2019. doi: 10.1109/WITS.2019.8723766.

[10] H. El Aimani and A. Essadki, "Study of the PI Controler and Sliding Mode of DFIG used in a WECS," 2018. doi: 10.1109/IRSEC.2017.8477248.

[11] Y. Boussairi, A. Abouloifa, I. Lachkar, C. Aouadi, and A. Hamdoun, "State Feedback Nonlinear Control Strategy for Wind Turbine System Driven by Permanent Magnet Synchronous Generator for Maximum Power Extraction and Power Factor Correction," *Vibration Analysis and Control in Mechanical Structures and Wind Energy Conversion Systems*, 2018, doi: 10.5772/intechopen.72366.

[12] O. Zamzoum, Y. El Mourabit, M. Errouha, A. Derouich, and A. El Ghzizal, "Power control of variable speed wind turbine based on doubly fed induction generator using indirect field-oriented control with fuzzy logic controllers for performance optimization," *Energy Science and Engineering*, vol. 6, no. 5, pp. 408–423, 2018, doi: 10.1002/ese3.215.

[13] S. Soman, N. Shelly, C. P. Kurian, and T. S. Sudheer Kumar, "DC transformer modeling and control of DC-DC buck converter," *International Journal of Power Electronics and Drive Systems*, vol. 10, no. 1, pp. 319–329, 2019, doi: 10.11591/ijpeds.v10.i1.pp319-329.

[14] C. Hamid *et al.*, "Performance improvement of the variable speed wind turbine driving a dfig using nonlinear control strategies," *International Journal of Power Electronics and Drive Systems*, vol. 12, no. 4, pp. 2470–2482, 2021, doi: 10.11591/ijpeds.v12.i4.pp2470-2482.

[15] A. Boukhriss, A. Essadki, A. Bouallouch, and T. Nasser, "Maximization of generated power from wind energy conversion systems using a doubly fed induction generator with active disturbance rejection control," *2014 2nd World Conference on Complex Systems, WCCS 2014*, pp. 330–335, 2015, doi: 10.1109/ICoCS.2014.7060907.

[16] A. Boukhriss, T. Nasser, and A. Essadki, "A Linear Active Disturbance Rejection Control applied for DFIG based Wind Energy Conversion System," 2013.

[17] I. Minka, A. Essadki, S. Mensou, and T. Nasser, "Power Control of a DFIG Driving by Wind Turbine: Comparison Study between ADRC and PI Controller," *Proceedings of 2017 International Renewable and Sustainable Energy Conference, IRSEC 2017*, vol. 1, no. 1, 2018, doi: 10.1109/IRSEC.2017.8477359.

[18] A. O. Simon, M. Guisser, E. Abdelmounim, M. Aboulfatah, H. Bahri, and L. Azeddine, "Multiple current sensor fault tolerant control of DFIG wind turbine," *2019 International Conference on Wireless Technologies, Embedded and Intelligent Systems, WITS 2019*, 2019, doi: 10.1109/WITS.2019.8723836.

[19] S. Abdelmalek, L. Barazane, and A. Larabi, "An advanced robust fault-tolerant tracking control for a doubly fed induction generator with actuator faults," 2017. doi: 10.3906/elk-1508-16.

[20] C. Hanene, B. S. Jihane, and K. Moufida, "A fault tolerant control for sensor and actuator failures of a non linear hybrid system," *International Journal of Electrical and Computer Engineering*, vol. 8, no. 5, pp. 2864–2882, 2018, doi: 10.11591/ijece.v8i5.pp2864-2882.

[21] A. Oumar, R. Chakib, and M. Cherkaoui, "Current Sensor Fault-Tolerant Control of DSIM Controlled by ADRC," 2020. doi: 10.1155/2020/6568297.

[22] S. Abdelmalek, L. Barazane, A. Larabi, and H. Belmili, "Contributions to diagnosis and fault tolerant control based on Proportional Integral Observer: Application to a doubly-fed induction generator," *2015 4th International Conference on Electrical Engineering, ICEE 2015*, 2016, doi: 10.1109/INTEE.2015.7416608.

[23] A. Amrane, A. Larabi, and A. Aitouche, "Fault detection and isolation based on nonlinear analytical redundancy applied to an induction machine," in *2017 6th International Conference on Systems and Control, ICSC 2017*, 2017, pp. 255–260. doi: 10.1109/ICoSC.2017.7958716.

[24] A. Djoudi, S. Bacha, and H. Iman-Eini, "Efficient real-time estimation for DFIG - Performance and reliability enhancement of grid/micro-grid connected energy conversion systems," 2019. doi: 10.1063/1.5058076.

[25] L. Zhou, J. Liu, and F. Liu, "Design and implementation of STATCOM combined with series dynamic breaking resistor for low voltage ride-through of wind farms," in *2010 IEEE Energy Conversion Congress and Exposition, ECCE 2010 - Proceedings*, 2010, pp. 2501–2506. doi: 10.1109/ECCE.2010.5617953.

[26] A. Boulmane, Y. Zidani, D. Belkhayat, and M. Bouchouirbat, "A GA-based adaptive mechanism for sensorless vector control of induction motor drives for urban electric vehicles," *Turkish Journal of Electrical Engineering and Computer Sciences*, vol. 28, no. 3, pp. 1731–1746, 2020, doi: 10.3906/elk-1910-39.

[27] C. Ahmed, A. Bekri, H. Gouabi, and H. Ali, "Non-Linear Back Stepping Control Optimized By Genetic Algorithm for the Control of a Wind Turbine," *International Journal of Industrial Electronics and Electrical Engineering*, vol. 7, no. 6, pp. 2347–2350, 2019.

BIOGRAPHIES OF AUTHORS

Ikram Aissaoui received a Specialized Master's Degree in industrial automation and quality control from Institut supérieur d'ingénierie et des affaires (ISGA), Rabat, Morocco, in 2018. She is currently preparing a PhD thesis in Research Center of Engineering and Health Sciences and Technologies (STIS), Ecole Nationale Supérieure d'Arts et Métiers (ENSAM), Mohammed V University in Rabat, Morocco. She can be contacted at email: ikraam.aissaoui@gmail.com.

Noureddine Elmouhi received the Engineer Degree in Electrical Engineering, from sciences and technologies Faculty (FST), Marrakesh, Morocco, in 2010. In 2023 he received his PhD thesis from Research Center of Engineering and Health Sciences and Technologies (STIS), Ecole Nationnale Supérieure d'Arts et Métiers (ENSAM), Mohammed V University in Rabat, Morocco. He can be contacted at email: n.elmouhi@gmail.com.

Ahmed Essadki is currently a professor and university research professor at the electrical engineering department of ENSAM, Mohammed V University Morocco**.** In 2000, he received his PhD degree from Mohammedia Engineering School (EMI), Morocco. From 1990 to 1993, he pursued his master program at UQTR university, Quebec Canada, respectively, all in electrical engineering. His current research interests include renewable energy, motor drives and power system. Dr ESSADKI is a member of RGE Lab in research group Leader. He can be contacted at email: ahmed.essadki1@gmail.com.

Hind Elaimani received the Master Degree in Electrical Engineering, from sciences and technologies Faculty (FST), Marrakesh, Morocco, in 2011. In 2023 he received his PhD thesis from Research Center of Engineering and Health Sciences and Technologies (STIS), Ecole Nationnale Supérieure d'Arts et Métiers (ENSAM), Mohammed V University in Rabat, Morocco. She can be contacted at email: h.elaimani@gmail.com.